Helix Packing in the Lactose Permease Determined by Metal−Nitroxide Interaction†

John Voss,‡ Wayne L. Hubbell,§ and H. Ronald Kaback*,‡

Howard Hughes Medical Institute, Departments of Physiology and Microbiology & Molecular Genetics, and Jules Stein Eye Institute and Department of Chemistry & Biochemistry, University of California at Los Angeles, Los Angeles, California 90095-1662

Received August 28, 1997; Revised Manuscript Received October 23, 1997⊗

ABSTRACT: The magnetic dipolar interaction between site-directed metal−nitroxide pairs can be exploited to measure distances within proteins [Voss, J., Salwinski, L., Kaback, H. R., and Hubbell, W. L. (1995) *Proc. Natl. Acad. Sci. U.S.A. 92*, 12295−12299; Voss, J., Hubbell, W. L., and Kaback, H. R. (1995) *Proc. Natl. Acad. Sci. U.S.A. 92*, 12300−12303], and the approach is utilized here to measure helix proximities in the lactose permease of *Escherichia coli*. A high-affinity divalent metal binding site was created by replacing Arg302 (helix IX) and Glu325 (helix X) with His residues in permease mutants containing single Cys residues in helices II, V, or VII and a biotin acceptor domain to facilitate purification. Mutant proteins were purified by avidin affinity chromatography, labeled specifically with a nitroxide free radical and investigated by electron paramagnetic resonance spectroscopy in the absence or presence of Cu(II). Spectral broadening due to bound Cu(II) was used to estimate distances between the metal center and the spin-labeled side chains. For each of the transmembrane domains probed, the variation in interspin distance with sequence position is consistent with an α-helical structure. The measured distances were also used to construct a model that is in good agreement with packing data obtained from other approaches.

The lactose permease (lac permease)[1] of *Escherichia coli* is a paradigm for secondary transport proteins that couple free energy stored in an electrochemical ion gradient into a solute concentration gradient (*1*−*5*). This polytopic membrane transport protein which catalyzes the coupled stoichiometric translocation of β-galactosides and H^+ (i.e., symport or cotransport) has been solubilized, purified, reconstituted, and shown to be solely responsible for β-galactoside transport [reviewed in Viitanen et al. (*6*)] as a monomer [see Sahin-Tóth et al. (*7*)]. All available evidence indicates that the permease is composed of 12 transmembrane helices connected by hydrophilic loops with the N- and C-termini on the cytoplasmic face (Figure 1).

With regard to helix packing, there are two pairs of interacting Asp and Lys residues that place helix VII close to helices X and XI (*8*−*14*). In addition, site-directed excimer fluorescence shows that helix VIII is close to helix X, helix IX is close to helix X, and helix X is in an α-helical conformation (*15*). Many of the spatial relationships have been confirmed by engineering divalent metal-binding sites (bis-His residues) within the permease. Permease with bis-His residues at positions 269 (helix VIII) and 322 (helix X), 302 (helix IX) and 325 (helix X), or 237 (helix VII) and 358 (helix XI) binds Mn(II) with a stoichiometry of unity, a K_D in the micromolar range, and an apparent pK_a of about 6.3 (*13*, *16*, *17*). Site-directed chemical cleavage confirms the positioning of helix X next to helices VII and XI and indicates further that helix V is close to helices VII and VIII (*18*). The relationship between helices V, VII, and VIII has been confirmed by site-directed spin-labeling and thiol cross-linking experiments (*19*). Site-directed cross-linking also demonstrates that helix I is close to helix VII, helix II is close to helices VII and XI (*20*) and helix VI is close to helix V (J. Wu and H. R. Kaback, unpublished observations). Finally, monoclonal antibody 4B11 binds to an epitope comprised of the last two cytoplasmic loops in the permease (*21*), thereby providing independent support for the close proximity between helices VIII−XI.

Site-directed spin-labeling (SDSL) is a valuable technique for investigating membrane protein structure and dynamics [reviewed in Hubbell and Altenbach (*22*, *23*)]. The method involves introduction of a single Cys residue into a protein devoid of native Cys residues, followed by labeling with a thiol-specific reagent containing a nitroxide spin-label. Studies of secondary structure and dynamics of membrane proteins are among the applications of SDSL (*22*−*24*), as well as measurement of distance between two paramagnetic centers (*19*, *25*−*31*). When the second paramagnetic center is another nitroxide, however, quantitative analysis of distance can be carried out only in the absence of motion or in the limit of fast motion where modulation of dipole−dipole interactions gives rise to relaxation effects. For higher molecular weights (≥15 000) and membrane proteins, the fast motional limit is not realized for interacting nitroxides, and quantitative analysis requires that conditions be arranged so that the spin system is in the slow motional limit which

†The research reported here was supported in part by NIH Grant DK51131 to H.R.K. and NIH Grant EY05216 and the Jules Stein Professorship Endowment to W.L.H.

* To whom correspondence and reprint requests should be addressed.

‡ Howard Hughes Medical Institute, Departments of Physiology and Microbiology & Molecular Genetics, 5-748 MRL, Box 951662, Los Angeles, CA 90095-1662.

§ Jules Stein Eye Institute and Department of Chemistry & Biochemistry.

⊗ Abstract published in *Advance ACS Abstracts,* December 15, 1997.

[1] Abbreviations: EPR, electron paramagnetic resonance; DPPH, 2,2-diphenyl-1-picrylhydrazyl; KP_i, potassium phosphate; SDS, sodium dodecyl sulfate; PCR, polymerase chain reaction; DM, 1-dodecyl-β-D-maltopyranoside.

S0006-2960(97)02152-1 CCC: $15.00
Published on Web 01/06/1998

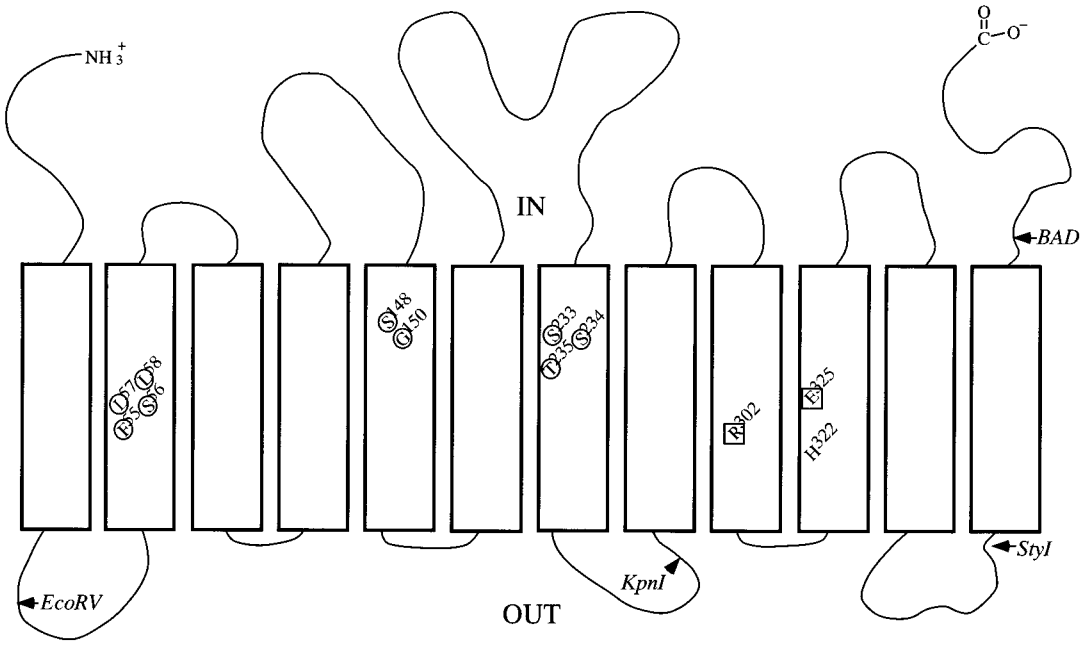

FIGURE 1: Secondary-structure model of Cys-less lac permease showing the Cys-substituted positions (circles) which were spin-labeled and the His-substituted residues (squares) comprising the Cu(II) binding site. Rectangles represent transmembrane helices. The location of restriction sites used for restriction fragment replacement and the site of the biotin acceptor domain (BAD) insertion are indicated with arrows.

is usually achieved by freezing. In addition to concerns regarding possible structural perturbations, freezing eliminates the possibility of studying dynamics. In this paper, an approach is used (*27*, *28*) that is based on the magnetic dipolar interaction between a spin-label and a paramagnetic metal ion. The method can be used under physiological conditions (i.e., at room temperature) and has been shown to provide reliable distances in T4 lysozyme, as well as lac permease.

Designed metal sites have provided confirmation of predicted spatial relationships among selected membrane-spanning domains of the lactose permease (*13*, *16*, *17*) as well as in G-protein-coupled receptors (*32*, *33*). With this strategy, predicted proximities are probed by measuring metal binding in a mutant with site-directed His substitutions. With lac permease, mutant R302H/E325H[2] which contains three His residues in close approximation (*13*) binds divalent metal with a stoichiometry of 1:1 and a K_D of about 10 μM. Using this engineered metal binding mutant in a Cys-less permease background, the metal−spin-label approach was used to estimate the distance and orientation of three helices with respect to the metal center. Individual Cys residues at positions 55−58 (helix II), 148 and 150 (helix V), and 233−235 (helix VII) were spin-labeled to generate nitroxide side chains, and EPR spectra were obtained in the absence or presence of Cu(II). The results confirm and extend helix proximity relationships obtained by other means.

EXPERIMENTAL PROCEDURES

Materials

(1-Oxy-2,2,5,5-tetramethylpyrrolinyl-3-methyl) methanethiosulfonate (methanethiosulfonate spin-label) was a gift from Kálmán Hideg and is available from Reanal (Budapest, Hungary) and Toronto Research Chemicals (Toronto, Ontario, Canada). Deoxyoligonucleotides were synthesized on an Applied Biosystems 391 DNA synthesizer. All restriction endonucleases and T_4 DNA ligase were from New England Biolabs, Beverly, MA. Sequenase was from United States Biochemical, Cleveland, OH. All other materials were reagent grade and obtained from commercial sources.

Methods

Construction, Expression, and Purification of Lac Permease Mutants. A lac permease mutant containing a metal-binding site (*13*) was constructed by two-stage polymerase chain reaction (PCR) to introduce the R302H and E325H mutations into Cys-less permease (*34*). Using this gene as a template, each single Cys mutant was engineered by restriction fragment replacement (*35*), making use of the restriction sites shown in Figure 1. In order to facilitate avidin affinity purification, the biotin acceptor domain from a *Klebsiella pneumoniae* oxaloacetate decarboxylase was then inserted into the C-terminus of each single Cys mutant (*36*). After the desired mutations were confirmed by dideoxynucleotide sequence analysis (*37*) preceded by alkali denaturation (*38*), *E. coli* T184 (*lacZ*$^-$*Y*$^-$) was transformed with plasmid encoding a given mutant. Cells were grown aerobically at 37 °C in LB broth with streptomycin (10 μg/mL) and ampicillin (100 μg/mL). Dense cultures were diluted 10-fold in a 12 L fermentor and allowed to grow for 2 h at 37 °C before induction with 0.5 mM iso-propyl 1-thio-β-D-galactopyranoside. After growth for another 2 h at 37 °C, cells were harvested and disrupted by passage through a French pressure cell. A membrane fraction was isolated by centrifugation and extracted with 3% DM, and permease was purified by affinity chromatography on immobilized monomeric avidin as described (*39*). Each purified mutant protein was then incubated with 100 μM (1-oxy-2,2,5,5-tetramethyl)methanethiosulfonate for 60 min at 4 °C to generate

[2] Site-directed mutants are designated by the single-letter amino acid abbreviation for the targeted residue, followed by the sequence position of the residue in the wild-type lac permease and then by a second letter indicating the amino acid replacement.

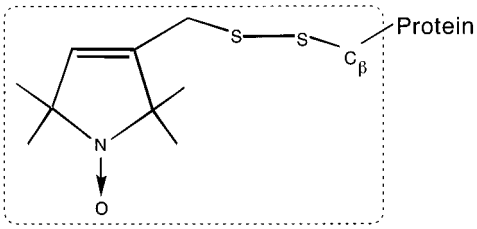

FIGURE 2: Structure of nitroxide side chain R1.

the nitroxide side chain R1 (Figure 2), concentrated, and dialyzed using a Micro-ProDiCon membrane (Spectrum) (*28*).

EPR Spectroscopy. EPR measurements were performed at 22 °C with given spin-labeled lac permease mutants in quartz capillaries. Samples (10 μL) of purified permease at a final concentration of ca. 60 μM in 10 mM MES (pH 7.5)/0.02% DM containing either 600 μM diamagnetic Zn(II) or paramagnetic Cu(II) were used for each measurement. Spectra were obtained using a Varian E-109 X-band spectrometer fitted with a loop-gap resonator (*40*, *41*) at a microwave power of 2 mW and a modulation amplitude optimized to the natural line width of the individual spectrum and recorded under field-frequency lock at X-band with a 100 G sweep at 30 s per scan. Spectra shown are composites from two separately prepared samples that were individually signal averaged over four scans.

Data Analysis. Spectral broadening due to dipolar interaction between a paramagnetic metal ion and a nitroxide was quantitated as described previously (*27*, *28*) by using a computer algorithm (*42*). Briefly, distance-dependent loss in nitroxide spectral intensity (I) due to the broadening influence of bound Cu(II) is observed. The amplitude of the broadened spectrum normalized to the unbroadened spectrum (I/I_0) is used to obtain C, the dipolar broadening coefficient as described in the equation

$$C = \frac{g\beta\mu^2\tau}{\hbar r^6} \qquad (1)$$

where g is the electronic g factor of the nitroxide, β is the Bohr magneton, μ is the magnetic moment of the metal, and r is the interspin distance. This treatment assumes that τ is equal to T_{1e},[3] the electronic relaxation time of the metal. Computer simulations of both isotropic and anisotropic line broadening were used to generate a plot of I/I_0 versus $C/\delta H_o$, where δH_o is the line width in the absence of broadening induced by the metal (*27*). From the plot, the experimental I/I_0 value is used to obtain a value for C, and the interspin distance is calculated from eq 1.

RESULTS

Helix II. Although F55R1, S56R1, L57R1, and L58R1 are ordered sequentially in the primary sequence of the permease, the line shapes of nitroxides at these positions differ (Figure 3). The spectra of S56R1, L57R1, and L58R1 permeases have a dominant broad component reflecting a motionally restricted spin population that arises most likely from tertiary interactions with other domains in the protein (*43*). On the other hand, the spectrum of F55R1 contains a significant population of highly mobile spins. The observations are consistent with previous findings (*20*, *44*) indicating that positions 56 and 57 are located on a face of helix II that is in close proximity to helices VII and IX and with the suggestion that F55R1 is directed away from the interior of the protein.

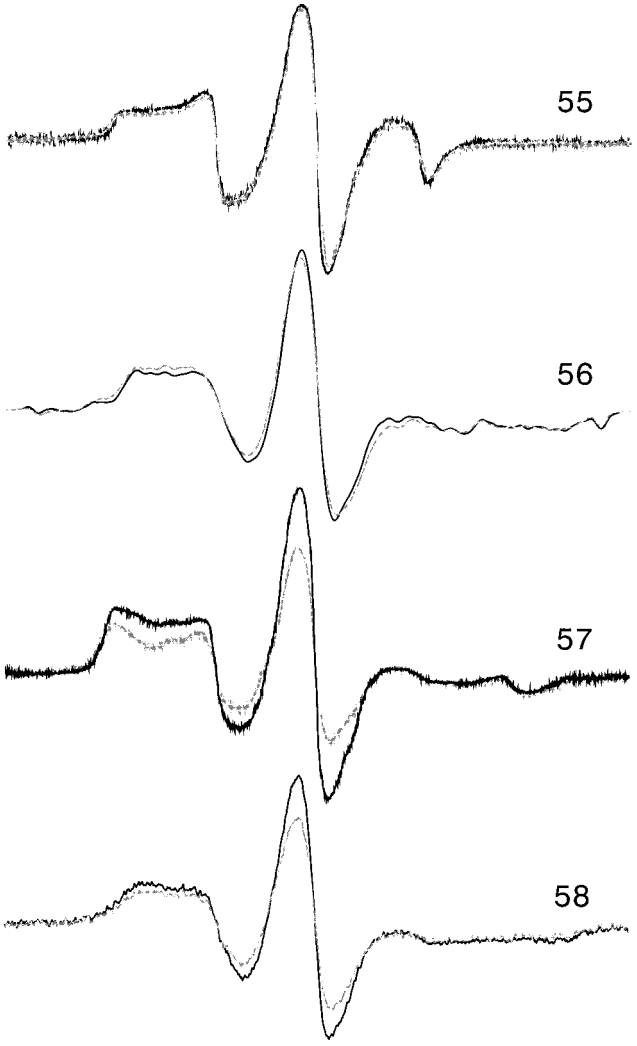

FIGURE 3: First-derivative EPR spectra of mutants F55R1, S56R1, L57R1, and L58R1 in helix II of the lac permease in the presence of either 600 μM Zn(II) (dark line) or 600 μM Cu(II) (light line). The magnetic field scan width is 98 G.

Cu(II) binding to a designed site in the same nitroxide-labeled protein results in distance-dependent broadening which can be quantitated from the reduction in amplitude of the center resonance line ($m_I = 0$) and used to calculate interspin distances (*27*, *28*). With permease mutants containing a tris-His divalent metal-binding site between helices VIII, IX, and X (*13*) and a given nitroxide-labeled side chain, Cu(II)-induced broadening of the center line is substantial at positions 57 and 58, but negligible at positions 55 and 56, demonstrating that positions 57 and 58 are closer to the Cu(II) site at the interface between helices VIII−X. The measurements are consistent with previous work (*20*, *44*) documenting the proximity and orientation of helix II with respect to helices VII−XI by thiol cross-linking. In addition, the calculated interspin distances between R1 on helix II and the metal center (Table 1) vary with sequence position in a manner consistent with that of an α-helix.

[3] T_{1e} is the spin−lattice relaxation time; T_{2e} is the transverse relaxation time.

Table 1: Spectral Parameters and Calculated Distances from Broadened R1 Spectra due to Cu(II) Binding to the R302H/E325H Site in Lac Permease[a]

mutant	I/I_0	δH_0 (G)	C	r (Å)
		Helix II		
F**55**R1	0.97 ± 0.05	4.2 ± 0.3	0.142 ± 0.4	>21[b]
S**56**R1	0.96 ± 0.05	5.3 ± 0.3	0.191 ± 0.4	>21
L**57**R1	0.62 ± 0.04	4.7 ± 0.3	2.64 ± 0.6	14 ± 1
L**58**R1	0.72 ± 0.03	5.0 ± 0.2	1.61 ± 0.4	15 ± 1
		Helix IV		
C**148**R1	0.74 ± 0.03	6.0 ± 0.2	2.04 ± 0.4	14 ± 1
G**150**R1	0.94 ± 0.04	4.1 ± 0.3	0.260	20 ± 1
		Helix VII		
S**233**R1	0.59 ± 0.04	5.2 ± 0.3	3.81 ± 0.7	12 ± 1
C**234**R1	0.75 ± 0.03	4.1 ± 0.2	1.30 ± 0.4	15 ± 1
T**235**R1	0.96 ± 0.04	4.7 ± 0.3	0.170 ± 0.4	>21

[a] The I/I_0 amplitudes represent the peak-to-peak magnitude of the center ($m_I = 0$) line normalized to the magnitude of the Zn(II) control. δH_0 represents the unbroadened center line width of the R1 spectra in the presence of Zn(II). C is the dipolar interaction coefficient and was obtained from simulated broadening of anisotropic spectra as described in Voss et al. (*27*). r is the interspin distance, rounded to the nearest angstrom, calculated from C as given by eq 1 in Methods. Errors in I/I_0 and δH_0 are estimated from the signal-to-noise ratio of the collected spectra and were propagated into the derived quantities C and r. [b] Where the Cu(II)−nitroxyl interaction is weak, distances greater than 21 Å cannot be accurately determined (*27*).

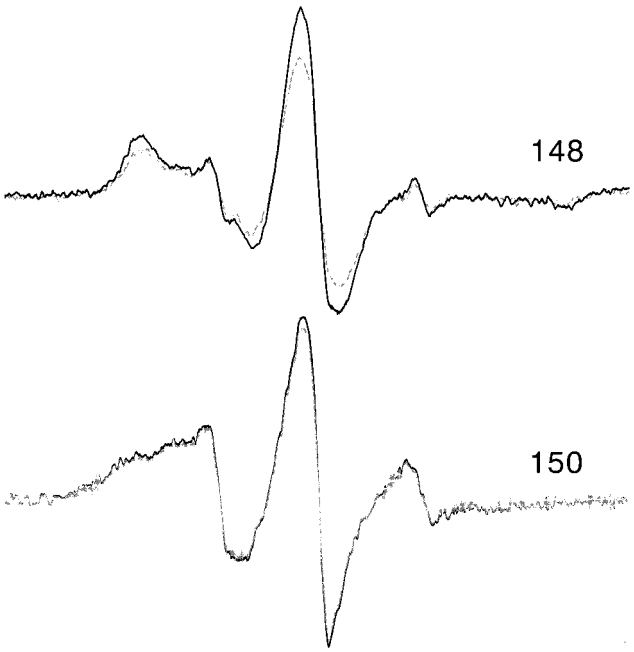

FIGURE 4: First-derivative EPR spectra of mutants C148R1 and G150R1 in helix V of the lac permease in the presence of either 600 μM Zn(II) (dark line) or 600 μM Cu(II) (light line). The magnetic field scan width is 98 G.

Helix V. EPR spectra of spin-labeled side chains C148R1 and G150R1 demonstrate dramatic differences in line shape (Figure 4). The spectrum of C148R1 reflects a side chain that is highly restricted, most likely due to a tight packing of the tertiary structure in this domain. However, the G150R1 line shape reflects much higher mobility, consistent with positioning on the exposed surface of a helix (*43*). The observations are consistent with previous findings (*18*−*20*, *44*) indicating that the face of helix V with Cys148 is oriented toward the interior of the protein.

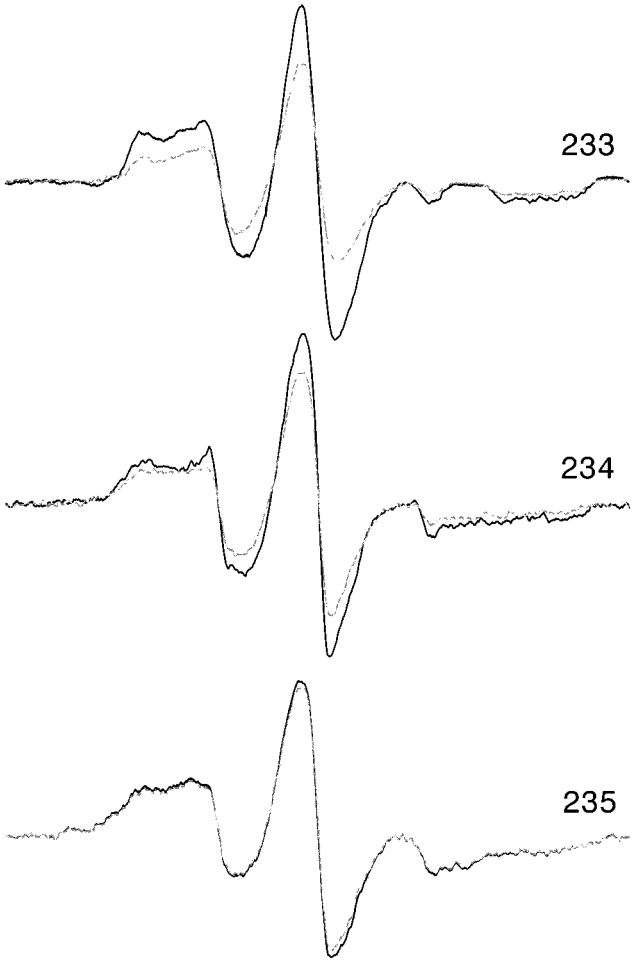

FIGURE 5: First-derivative EPR spectra of mutants S233R1, C234R1, and T235R1 in helix VII of the lac permease in the presence of either 600 μM Zn(II) (dark line) or 600 μM Cu(II) (light line). The magnetic field scan width is 98 G.

Cu(II)-induced broadening is substantial at position 148, but negligible at position 150 (Figure 4, Table 1), demonstrating that position 148 is closer to the Cu(II) site. Again, the observations are consistent with earlier work in which the proximity and orientation of helix V with respect to helices VII−XI were studied by other means (*18*, *19*). In addition, the large difference in broadening between positions 148 and 150 in the presence of Cu(II) is consistent with these residues being oriented in opposite directions, thereby providing further evidence that transmembrane domain V is in an α-helical conformation.

Helix VII. Spectra of permease with S233R1, C234R1, or T235R1 exhibit line shapes that reflect relatively immobilized side chains (Figure 5), a finding that supports other data indicating that helix VII neighbors other transmembrane domains (*45*). Moreover, Cu(II)-induced broadening is substantial at positions 233 and 234, but insignificant at position 235 (Figure 5, Table 1), indicating that T235R1 is oriented away from the Cu(II) site at the interface of helices VIII−X. The observations are consistent with an orientation of helix VII with Asp237 directed towards helix XI and Asp240 directed toward helix X (*46*).

DISCUSSION

By using a battery of site-directed techniques which include site-directed mutagenesis and chemical modification,

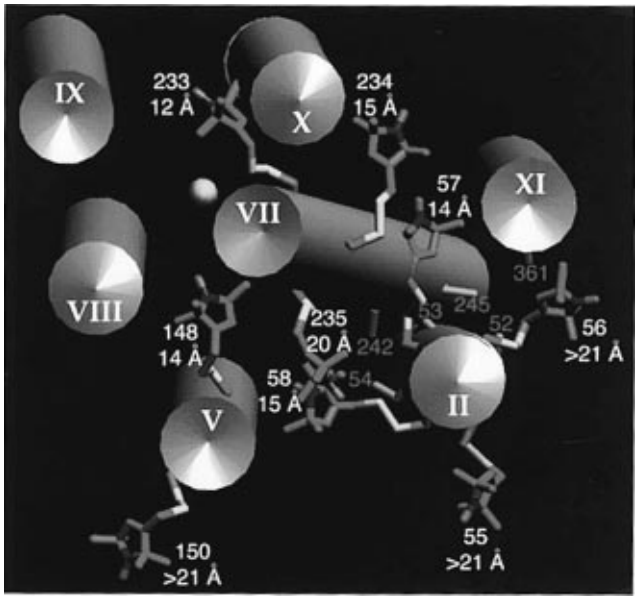

FIGURE 6: Molecular model of helix packing in the lactose permease with distances obtained from Cu(II)−nitroxide measurements. Helices are represented as solid gray rods. Shown is the engineered metal binding site (R302H/E325H/His322) (*13*) in combination with nitroxide side chains at F55C, S56C, L57C, and L58C (helix II); 148C and G150C (helix V); and S233C, 234C, and T235C (helix VII). Each spin-labeled mutant was studied individually in a Cys-less background. The helix packing model is derived from the measurements obtained here and from previously published data (see text). Approximate interspin distances were determined from nitroxide spectral broadening (Table 1). The model was constructed using Insight software from Biosym Inc. The distances given represent an average distance separating a population of interacting metal−nitroxide dipoles (*27*). Obviously, distances may vary from the average depending upon dynamics within the structure. The spin-labeled side chains in helices V and VII are closer to the cytoplasmic surface of the membrane, while the substituted positions in helix II are at about the same depth as the metal ion binding site (i.e., near the bilayer center). Also indicated in orange are the Cys replacements studied by chemical cross-linking (*20*, *44*) which are located near the periplasmic ends of helices II, VII, and XI.

excimer fluorescence, engineered divalent metal-binding sites, chemical cleavage, EPR, thiol cross-linking, and identification of discontinuous monoclonal antibody epitopes, a helix-packing model for lac permease has been formulated [reviewed in Kaback et al. (*45*)]. Using a portion of this scheme, a molecular model was generated according to the calculated interspin distances obtained from the Cu(II)-broadened nitroxide spectra with each spin-labeled permease mutant (Figure 6). To construct the 3-D molecular model, the position and orientation of the helices, as well as the tilt of helix VII (see below), were adjusted to satisfy proximities obtained from both interspin distances and previous observations.

The model presented in Figure 6 is a view of the helices from the cytoplasmic surface. While the lateral separation between sites is readily apparent, the vertical position of the R1 side chains with respect to the Cu(II) ion which is near the bilayer center is more difficult to discern. For instance, since C148R1 is near the cytoplasmic end of helix V, the actual distance to the bound Cu(II) is greater than it appears to be in the model. Positions 233, 234, and 235 in helix VII are midway between the bilayer center and the cytoplasm (*47*), while the spin-labeled positions in helix II are predicted to lie at about the same depth as the Cu(II) binding site. Therefore, while the axis of helix VII occupies the space between helix II and the metal center, positions 57 and 58 are sufficiently close to the Cu(II) that the signals from the nitroxide side chains are altered.

The distances given in Table 1 and illustrated in Figure 6 are consistent with information obtained from a variety of other approaches (*15*, *18*−*21*, *44*, *45*). Of particular note are recent cross-linking studies by Wu and Kaback (*20*, *44*) which probe distances between Cys residues on helix II and Cys residues on helices VII or XI. In the packing model presented here, the relative orientation of helix II is rotated approximately 90° clockwise relative to the bound Cu(II) when compared to other packing representations [see Kaback et al. (*45*)]. However, by incorporating the tilt of helix VII (*47*), the model presented here is remarkably consistent with interhelical distances determined by chemical cross-linking. Thus, a Cys residue at position 245 (helix VII) cross-links with a Cys residue at either position 52 or position 53 (helix II), but not with a Cys residue at position 54 (*20*), and position 245 is approximately equidistance from positions 52 and 53 (*44*). The observation that position 242 (helix VII) cross-links with position 53 (helix II), but not position 52, is also consistent with the model. Similarly, the distance between position 245 and position 52 or 53 is less than the distance between positions 242 and 53, which cross-link more weakly, and positions 52 and 53 are closer to position 245 than position 361 as judged both by cross-linking (*20*, *44*) and the model presented here.

The metal−spin-label technique provides further information on the relative orientation of helical faces in the permease, thereby facilitating determination of contacts between these faces. In addition, the distances obtained are consistent with the placement of the spin-labeled side chains in α-helices, thereby providing further evidence that transmembrane domains II, V, and VII are indeed in α-helical conformation. Dynamic information is also obtained from spectral line shapes. Interior sites are expected to be more immobilized, resulting in a broad signature EPR spectrum (*24*, *43*, *48*). On the basis of this criterion, the results obtained here are also consistent with the model. For example, mutants G150R1 and F55R1 which are predicted to point away from the protein interior exhibit the most mobile spectra. Although the model shown illustrates packing for 7 of the 12 helices, recent cross-linking studies (*20*) place helix I near the interface between helices II and VII and helix XII in close proximity to helices II and XI (*49*). Thus the face of helix II containing S56R1, a position with a moderately immobilized line shape, is probably facing another part of the protein rather than the lipid bilayer.

A concern of site-directed spectroscopy is the effect of a given mutation and subsequent labeling on the native structure. The objective of these studies is to resolve structure to the level of helix packing, and it is unlikely that changes resulting from introduction of the probe drastically change the backbone positions of the helices. The functional importance of all 417 residues in the permease has been studied by site-directed and Cys-scanning mutagenesis (*46*, *50*), and only six residues are irreplaceable with respect to active lactose transport [Glu126 (helix IV), Arg144 (helix V), Glu269 (helix VIII), Arg302 (helix IX), and His322 and Glu325 (helix X)]. While the R302H/E325H metal-binding mutant is inactive, several lines of evidence [reviewed in

Kaback (*3*, *46*) and Kaback et al. (*45*)] are consistent with the argument that Arg302 and Glu325 are in close proximity in the native enzyme. Since binding of divalent metal (in this case, either Zn^{2+} or Cu^{2+}) necessitates close proximity between positions 302 and 325, the mutants examined here are likely to approximate the native conformation of this domain. In addition, to further probe the tolerance of the permease to side chain perturbation, the sensitivity of Cys replacements to modification by *N*-ethylmaleimide has been determined at each position in the protein, including the positions spin-labeled here (*51*−*53*). Except for Cys148, each Cys mutant used in this study retains significant activity even after modification with *N*-ethylmaleimide. Cys148, a substrate-binding residue (*54*, *55*), has been modified by a variety of spectroscopic probes, chemical cross-linkers, and *o*-phenanthroline−Cu^{2+}, a chemical cutting reagent. The results from these studies indicate that although permease alkylated at Cys148 cannot bind substrate, it retains near-native structure in other aspects.

ACKNOWLEDGMENT

We are grateful for the excellent technical assistance provided by Leslie Wang.

REFERENCES

1. Kaback, H. R. (1976) *J. Cell. Physiol. 89*, 575−593.
2. Kaback, H. R. (1983) *J. Membr. Biol. 76*, 95−112.
3. Kaback, H. R. (1997) *Proc. Natl. Acad. Sci. U.S.A. 94*, 5539−5543.
4. Poolman, B., and Konings, W. N. (1993) *Biochim. Biophys. Acta 1183*, 5−39.
5. Varela, M. F., and Wilson, T. H. (1996) *Biochim. Biophys. Acta 1276*, 21−34.
6. Viitanen, P., Garcia, M. L., and Kaback, H. R. (1984) *Proc. Natl. Acad. Sci. U.S.A. 81*, 1629−1633.
7. Sahin-Tóth, M., Lawrence, M. C., and Kaback, H. R. (1994) *Proc. Natl. Acad. Sci. U.S.A. 91*, 5421−5425.
8. King, S. C., Hansen, C. L., and Wilson, T. H. (1991) *Biochim. Biophys. Acta 1062*, 177−186.
9. Sahin-Tóth, M., Dunten, R. L., Gonzalez, A., and Kaback, H. R. (1992) *Proc. Natl. Acad. Sci. U.S.A. 89*, 10547−10551.
10. Lee, J. L., Hwang, P. P., Hansen, C., and Wilson, T. H. (1992) *J. Biol. Chem. 267*, 20758−20764.
11. Dunten, R. L., Sahin-Toth, M., and Kaback, H. R. (1993) *Biochemistry 32*, 3139−3145.
12. Sahin-Tóth, M., and Kaback, H. R. (1993) *Biochemistry 32*, 10027−10035.
13. He, M. M., Voss, J., Hubbell, W. L., and Kaback, H. R. (1995) *Biochemistry 34*, 15667−15670.
14. Frillingos, S., and Kaback, H. R. (1996) *Biochemistry 35*, 13363−13367.
15. Jung, K., Jung, H., Wu, J., Privé, G. G., and Kaback, H. R. (1993) *Biochemistry 32*, 12273−12278.
16. Jung, K., Voss, J., He, M., Hubbell, W. L., and Kaback, H. R. (1995) *Biochemistry 34*, 6272−6277.
17. He, M. M., Voss, J., Hubbell, W. L., and Kaback, H. R. (1995) *Biochemistry 34*, 15661−15666.
18. Wu, J., Perrin, D., Sigman, D., and Kaback, H. (1995) *Proc. Natl. Acad. Sci. U.S.A. 92*, 9186−9190.
19. Wu, J., Voss, J., Hubbell, W. L., and Kaback, H. R. (1996) *Proc. Natl. Acad. Sci. U.S.A. 93*, 10123−10127.
20. Wu, J., and Kaback, H. R. (1996) *Proc. Natl. Acad. Sci. U.S.A. 93*, 14498−15502.
21. Sun, J., Li, J., Carrasco, N., and Kaback, H. R. (1997) *Biochemistry 36*, 274−280.
22. Hubbell, W. L., and Altenbach, C. (1994) *Curr. Opin. Struct. Biol. 4*, 566−573.
23. Hubbell, W. L., and Altenbach, C. A. (1994) in *Membrane protein structure* (White, S. H., Ed.) pp 224−248, Oxford University Press, New York.
24. Voss, J., He, M., Hubbell, W., and Kaback, H. R. (1996) *Biochemistry 35*, 12915−12918.
25. Hustedt, E. J., Smirnov, A. I., Laub, C. E., Cobb, C. E., and Beth, A. H. (1997) *Biophys. J. 74*, 1861−1877.
26. Anthony-Cahill, S. J., Benfield, P. A., Fairman, R., Wasserman, Z. R., Brenner, S. L., Stafford, W. D., Altenbach, C., Hubbell, W. L., and DeGrado, W. F. (1992) *Science 255*, 979−983.
27. Voss, J., Salwinski, L., Kaback, H. R., and Hubbell, W. L. (1995) *Proc. Natl. Acad. Sci. U.S.A. 92*, 12295−12299.
28. Voss, J., Hubbell, W. L., and Kaback, H. R. (1995) *Proc. Natl. Acad. Sci. U.S.A. 92*, 12300−12303.
29. Rabenstein, M. S., and Shin, Y.-K. (1995) *Proc. Natl. Acad. Sci. U.S.A. 92*, 8239−8243.
30. Farrens, D. L., Altenbach, C., Yang, K., Hubbell, W. L., and Khorana, H. G. (1996) *Science 274*, 768−770.
31. Mchaourab, H. S., Oh, K. J., Fang, C. J., and Hubbell, W. L. (1997) *Biochemistry 36*, 307−316.
32. Elling, C. E., Nielsen, S. M., and Schwartz, T. W. (1995) *Nature 374*, 74−77.
33. Sheikh, S. P., Zvyaga, T. A., Lichtarge, O., Sakmar, T. P., and Bourne, H. R. (1996) *Nature 383*, 347−350.
34. van Iwaarden, P. R., Pastore, J. C., Konings, W. N., and Kaback, H. R. (1991) *Biochemistry 30*, 9595−9600.
35. Frillingos, S., Sahin-Toth, M., Persson, B., and Kaback, H. R. (1994) *Biochemistry 33*, 8074−8081.
36. Consler, T. G., Persson, B. L., Jung, H., Zen, K. H., Jung, K., Prive, G. G., Verner, G. E., and Kaback, H. R. (1993) *Proc. Natl. Acad. Sci. U.S.A. 90*, 6934−6938.
37. Sanger, F., Nicklen, S., and Coulsen, A. R. (1977) *Proc. Natl. Acad. Sci. U.S.A. 74*, 5463−5467.
38. Hattori, M., and Sakaki, Y. (1986) *Anal. Biochem. 152*, 1291−1297.
39. Wu, J., Frillingos, S., Voss, J., and Kaback, H. R. (1994) *Protein Sci. 3*, 2294−2301.
40. Froncisz, W., and Hyde, J. S. (1982) *J. Magn. Reson. 47*, 515−521.
41. Hubbell, W. L., Froncisz, W., and Hyde, J. S. (1987) *Rev. Sci. Instrum. 58*, 1879−1886.
42. Leigh, J. S. (1970) *J. Chem. Phys. 52*, 2608−2612.
43. Mchaourab, H., Lietzow, M. A., Hideg, K., and Hubbell, W. L. (1996) *Biochemistry 35*, 7692−7704.
44. Wu, J., and Kaback, H. R. (1997) *J. Mol. Biol. 270*, 285−293.
45. Kaback, H. R., Voss, J., and Wu, J. (1997) *Curr. Opin. Struct. Biol. 7*, 537−542.
46. Kaback, H. R. (1996) in *Handbook of Biological Physics: Transport Processes in Eukaryotic and Prokaryotic Organisms* (Konings, W. N., Kaback, H. R., and Lolkema, J. S., Eds.) pp 203−227, Elsevier, Amsterdam.
47. Voss, J., Hubbell, W. L., Hernandez, J., and Kaback, H. R. (1997) *Biochemistry* (submitted for publication).
48. Hubbell, W. L., Mchaourab, H. A., Altenbach, C., and Lietzow, M. A. (1996) *Structure 4*, 779−783.
49. Sun, J., and Kaback, H. R. (1997) *Biochemistry* (in press).
50. Frillingos, S., Gonzalez, A., and Kaback, H. R. (1997) *Biochemistry* (in press).
51. Frillingos, S., and Kaback, H. R. (1996) *Biochemistry 35*, 3950−3956.
52. Frillingos, S., Sun, J., Gonzalez, A., and Kaback, H. R. (1997) *Biochemistry 36*, 269−273.
53. Frillingos, S., Wu, J., Venkatesan, P., and Kaback, H. R. (1997) *Biochemistry 36*, 6408−6414.
54. Jung, H., Jung, K., and Kaback, H. R. (1994) *Biochemistry 33*, 12160−12165.
55. Wu, J., and Kaback, H. R. (1994) *Biochemistry 33*, 12166−12171.

BI972152L